ISSN: 2476-6909; Modares Mechanical Engineering. 2024;24(10):643-655.

Passive Vibration Control of a Nonlinear Rotating Beam Using a Nonlinear Vibration Absorber and Stability Analysis

ARTICLE INFO

Article Type
Original Research

Authors
Tangsiri A.[1],
Karamooz Mahdiabadi M.[1*],
Bab S.[2],

How to cite this article
Tangsiri A, Karamooz Mahdiabadi M, Bab S. Passive Vibration Control of a Nonlinear Rotating Beam using a Nonlinear Vibration Absorber and Stability Analysis. Modares Mechanical Engineering; *2024;24(10):643-655.*

ABSTRACT

Passive vibration control of rotating nonlinear beams is crucial due to its potential to mitigate harmful vibrations in various engineering applications, including aerospace and industrial sectors. This study examines how different system parameters and inherent nonlinearities influence the vibrations of a nonlinear rotating beam subjected to periodic external forces. A nonlinear energy sink (NES) is attached to the beam's tip to attenuate vibrations. The system is modeled using the Euler-Bernoulli beam theory and von Kármán strain-displacement relations, with equations of motion derived via Hamilton's principle. Complexification Averaging and Runge-Kutta methods are applied for analytical and numerical solutions, respectively. The findings reveal that increasing the stiffness reduces vibration amplitude, while a rise in the nonlinear coefficient induces hardening behavior. The system exhibits saddle-node and Hopf bifurcations under certain conditions, indicating complex dynamic transitions. These phenomena, driven by the beam's nonlinearity and the NES, effectively diminish the vibration amplitude, highlighting the system's complex dynamic responses and the NES's efficacy in vibration mitigation.

Keywords Rotating Nonlinear Beam, Nonlinear Energy Sink, Vibration Mitigation, Saddle-Node Bifurcations, Hopf Bifurcations.

[1] Tarbiat Modares University, Tehran. Iran
[2] Niroo Research Institute, Tehran, Iran

Correspondence
Address: Tarbiat Modares University, Tehran. Iran

karamooz@modares.ac.ir

Article History
Received: November 5, 2024
Accepted: November 27, 2024
ePublished: January 21, 2025

CITATION LINKS

1- Vibration mitigation of a rotating beam under external periodic force using ... 2- Vibration control of a pre-twisted rotating beam with nonlinear bi-stable attachments. 3- On the analysis of a passive vibration absorber for ... 4- Exact Nonlinear Dynamic Analysis of a Beam with a Nonlinear Vibration Absorber and ... 5- Vibration analysis of beam structures with ... 6- Vibration suppression and dynamic behavior analysis of ... 7- Modal Reduction of a Nonlinear Rotating Beam Through Nonlinear Normal Modes. 8- Natural frequencies of rotating twisted beams: a perturbation method-based approach. 9- Flap-wise vibrations of non-uniform rotating cantilever beams... 10- Vibration suppression of nonlinear rotating metamaterial beams. 11- Vibration control of a rotating Timoshenko beam-tendon system via ... 12- Passivity-based control of nonlinear active dynamic vibration absorber. 13- Vibration suppression of a geometrically nonlinear beam with boundary inertial nonlinear energy sinks. 14- Performances of dynamic vibration absorbers for beams subjected to moving loads. 15- Inplane vibration analysis of rotating beams with elastic restraints 16- Vibration suppression of a rotating functionally graded beam with enhanced active constrained layer damping treatment in temperature field. 17- Fundamentals of vibrations. 18- The mechanics of nonlinear systems with internal resonances. 19- Applications of Nonlinearity in Passive Vibration Control: A Review. 20- Parameters optimization of a nonlinear dynamic absorber for a nonlinear system. 21- Design and validation of a nonlinear vibration absorber to attenuate torsional oscillations of propulsion systems. 22- Nonlinear magnetic vibration absorber for passive control of a multi–storey structure. 23- Non-linear vibration and bifurcation analysis of Euler-Bernoulli beam under parametric excitation 24- Vibration suppression of rotating beams using time-varying internal tensile force. 25- Analysis of a Nonlinear Dynamic Vibration Absorber. 26- Application of a dynamic vibration absorber to a piecewise linear beam system under pre-tension. 27-Applied nonlinear dynamics: analytical, computational, and experimental methods

1- Introduction

The study of vibration control in rotating beams is critical because it has numerous applications in many engineering fields, including aerospace, mechanical, and civil engineering. Complex dynamic loading conditions can cause significant vibrations in rotating beams in helicopter blades and wind turbines. If not addressed properly, these vibrations can cause structural fatigue, decreased performance, and even catastrophic failure. As a result, effective vibration control strategies are required to ensure the reliability and longevity of these systems.

The simplicity, reliability, and energy-saving qualities of passive vibration control techniques make them particularly appealing. The majority of these methods employ dynamic vibration absorbers. Traditional linear DVAs may not be sufficient for systems with large deflections, material nonlinearities, or other nonlinear dynamic effects. Nonlinear vibration absorbers have been proposed as a more effective alternative to controlling vibrations in nonlinear systems to address these challenges.

Recent studies indicate that Nonlinear Vibration Absorbers (NVAs) can greatly enhance vibration reduction in systems exhibiting nonlinear behaviors. For instance, Bab et al. investigated the vibration mitigation of a rotating beam with a Nonlinear Energy Sink (NES), under external periodic forces to demonstrat the NES's ability to mitigate vibration across a broad frequency range, thus reducing resonant vibrations effectively [1]. Similarly Bera et al. Investigated vibration control in a twisted rotating beam with nonlinear bi stable attachments highlighting how the absorbers nonlinear features enhance vibration suppression [2].

Abdollahi et al. Delved into designing vibration absorbers for submerged beams under forces offering insights on optimizing absorber parameters for effective vibration control in nonlinear fluid structure interactions [3]. Bukhari and Barry conducted a dynamic analysis of a beam with a nonlinear vibration absorber under different boundary conditions underscoring the influence of boundary conditions on the systems vibrational behavior [4]. Chouvion examined the vibration analysis of beams with localized nonlinearities using a wave based approach revealing the impact of localized nonlinearities, on the response of structures [5]. Zhao et al. studied how a beam, under load behaves when equipped with a Nonlinear Energy Sink (NES) and supported by types of boundaries [6].

In the realm of rotating beams Pesheck and colleagues devised a method to simplify the analysis of vibrating systems by reducing the required number of modes through normal modes (NNMs) for nonlinear rotating beams [7]. Baxy and Sarkar examined the natural frequencies of rotating twisted beams using a perturbation method, providing critical insights for predicting and mitigating resonant conditions in rotating structures [8]. Huang et al. present an experimental study of the flap-wise vibration of three rotating beams with different cross-section patterns under different speeds, providing valuable experimental data for the analysis of flap-wise vibrations of non-uniform rotating cantilever beams [9].

Moreover, Basta et al. Explored vibration suppression, in rotating beams showcasing how metamaterials can enhance passive damping in nonlinear systems [10]. Wu and Titurus studied vibration control in a Timoshenko beam tendon system by integrating guiding inerter dampers introducing an approach that utilizes inerter devices to improve damping performance [11].

Various research studies have looked into incorporating Nonlinear Vibration Absorbers (NVAs) into rotating systems. Hao and colleagues proposed a control strategy based on passivity, for dynamic vibration absorbers shedding light on how control methods can be customized to the nonlinear characteristics of the system to optimize vibration reduction [12]. Zhang et al. investigated the vibration suppression of a geometrically nonlinear beam with boundary inertial nonlinear energy sinks, emphasizing the importance of boundary conditions in enhancing vibration control [13].

Further contributions to the field include Samani et al. who studied the performance of dynamic vibration absorbers for beams subjected to moving loads, particularly relevant in contexts such as bridges or rails where loads are not static [14]. Wang et al. Scrutinized in plane vibrations of rotating beams with restraints offering insights into how boundary conditions and elastic supports impact vibrational patterns [15]. Fang et al. Scrutinized in plane vibrations of rotating beams with restraints offering insights into how boundary conditions and elastic supports impact vibrational patterns [16].

Foundational studies have also played a significant role in advancing this field. Meirovitch provided a key text on vibration theory, both linear and nonlinear, and its applications across various engineering domains [17]. Manevich and Manevich delved into the mechanics of nonlinear systems with internal resonances, a crucial concept for understanding the complex interactions within nonlinear vibrating systems [18].

The relevance of nonlinearity in passive vibration control is further highlighted in Balaji and SelvaKumar, which reviewed various nonlinear strategies and their effectiveness in different engineering applications, underlining the growing importance of nonlinear methods in vibration control [19]. Nazari and Rahi focused on optimizing parameters for a nonlinear dynamic absorber in a nonlinear system, emphasizing the need to tailor absorber properties to the specific nonlinear characteristics of the system for enhanced performance [20].

Additionally, Haris et al. designed and validated a nonlinear vibration absorber to attenuate torsional oscillations in propulsion systems, demonstrating the practical application of NVAs in critical engineering systems [21]. Feudo et al. introduced a nonlinear magnetic vibration absorber for passive control of multi-story structures, showcasing the versatility of NVAs in different structural contexts [22]. Liao provided a comprehensive analysis of non-linear vibration and bifurcation in Euler-Bernoulli beams under parametric excitation, further expanding the understanding of nonlinear dynamics in beam structures [23].

Younesian and Esmailzadeh investigated the use of time-varying internal tensile forces for vibration suppression in rotating beams, allowing for dynamic adjustment of the tensile forces to mitigate vibrations effectively [24]. Pipes in a classic study, provided an early analysis of nonlinear dynamic

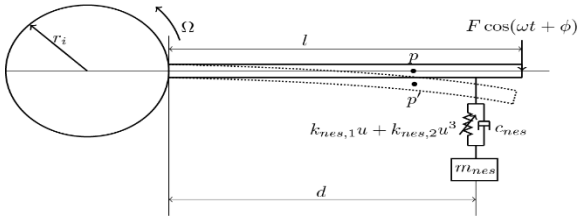

Fig. 1) The rotating nonlinear beam to which NES is attached.

vibration absorbers, laying the groundwork for subsequent research in this area [25]. Finally, de Bruin explored the application of dynamic vibration absorbers to piecewise linear beam systems under pre-tension, offering insights into the challenges and opportunities of using DVAs in complex nonlinear systems [26].

This article seeks to expand on research by studying how a nonlinear rotating beam can be passively controlled for vibration using a Nonlinear Energy Sink (NES) attached to the tip of the beam. The research delves into how system parameters and nonlinear interactions affect the vibrations of the beam when subjected to forces around the 1:1 resonance of its first natural frequency. By applying Euler Bernoulli beam theory and von Karman strain displacement relations the study models the dynamics of the rotating beam. Derives equations of motion using Hamilton's principle. Through the use of Complexification Averaging method and Runge Kutta method, for analysis valuable insights are gained that enhance both knowledge of nonlinear dynamics in rotating beams and practical applications in developing effective vibration control systems. The study also conducts an analysis with research like that of Bob et al. [1] focusing on rotating beams showcasing the performance of NES in nonlinear situations and its broader impact on reducing vibrations in important industrial equipment such, as gas turbines, helicopter rotors and wind turbine blades.

2- *Equations of Motion*

Consider a beam that is radially attached to a rotating disc. An angular velocity Ω is imposed on the disc (Ref. to figure 1). The rotating beam is modeled using Euler-Bernoulli beam theory and the centrifugal stiffening effect is considered. A point p on the beam at a radius r, which shifts to position p' due to vibration. The displacement of this point within the plane of rotation is represented by v. The coordinates of point p' in the rotating and inertial frame are present as:

$$R=\begin{pmatrix} r\,cos(t\Omega)-v\,sin(t\Omega)\\ r\,sin(t\Omega)+v\,cos(t\Omega)\end{pmatrix} \tag{1}$$

If we assume that the speed of rotation is constant and differentiate the coordinate expressions with respect to time, we can readily calculate the velocity of point p as:

$$\begin{aligned} V&=\dot{R}\\ &=\begin{pmatrix}-r\Omega\,sin(t\Omega)-v\Omega\,cos(t\Omega)-\dot{v}\,sin(t\Omega)\\ r\Omega\,cos(t\Omega)-v\Omega\,sin(t\Omega)+\dot{v}\,cos(t\Omega)\end{pmatrix}\end{aligned} \tag{2}$$

The locations of the NES mass are shown as follows:

$$\begin{aligned} &R_d\\ &=\begin{pmatrix} r\,sin(\Omega t)-v\,cos(\Omega t)-u\,cos(\Omega t)\\ r\,cos(\Omega t)+v\,sin(\Omega t)+u\,sin(\Omega t)\end{pmatrix}\delta\big(r\\ &-(r_i+d)\big)\end{aligned} \tag{3}$$

Based on the velocity, the kinetic energy of the system including beam and NES can be represented by the following expression:

$$T=\frac{1}{2}\rho AV^TV+\frac{1}{2}m_{nes}\dot{R}_d{}^T\dot{R}_d \tag{4}$$

According to the principles of nonlinearity as outlined in Von Kármán's seminal theory, the strain and stress fields within a beam structure can be comprehensively described by the following set of equations:

$$\varepsilon_{xx}=\frac{1}{2}v'^2-yv'' \tag{5}$$

$$\sigma_{xx}=\varepsilon_{xx}E=E\left(\frac{1}{2}v'^2-yv''\right) \tag{6}$$

The strain energy of the beam and nonlinear spring is given by the expression below:

$$\begin{aligned} U&=\frac{1}{2}\varepsilon_{xx}\sigma_{xx}+\delta\big(r-(r_i+d)\big)\left(\frac{1}{2}k_{nes,1}u^2\right.\\ &\qquad\left.+\frac{1}{4}k_{nes,2}u^4\right)\\ &=\delta\big(r-(r_i+d)\big)\left(\frac{1}{2}k_{nes,1}u^2+\frac{1}{4}k_{nes,2}u^4\right)\\ &+\frac{1}{8}Ev'^4-\frac{1}{2}yEv'^2v''+\frac{1}{2}y^2Ev''^2\end{aligned} \tag{7}$$

The centrifugal force, an inherent result of rotational motion, is axially applied to the beam as follows:

$$p(r)=\frac{1}{2}\rho A\Omega^2({r_o}^2-r^2) \tag{8}$$

The strain energy, which is induced by the centrifugal force, can be articulated as follows:

$$U_r=\frac{1}{4}(-r^2+{r_0}^2)A\rho\Omega^2v'^2 \tag{9}$$

The work influenced by neoconservative forces can be achieved in the following manner:

$$\begin{aligned} &\delta W_{nc}\\ &=\begin{pmatrix}-c_b\dot{v}+\delta(l-r+r_i)F\,cos(\phi+t\omega)\\ -c_{nes}\delta(d-r+r_i)(\dot{u})\end{pmatrix}^T\begin{pmatrix}\delta v\\ \delta u\end{pmatrix}\end{aligned} \tag{10}$$

Drawing upon Hamilton's principle, the equations of motion for the system can be derived as:

$$\int_{t_1}^{t_2}(\delta T-\delta U-\delta U_r+\delta W_{nc})dt=0 \tag{11}$$

$$A\rho\ddot{v} - A\rho\Omega^2 v + \frac{1}{2}A\rho\Omega^2\left(2rv' + (r^2 - {r_o}^2)v''\right) - \frac{3}{2}E{v'}^2v'' + IEv'''' + c_b\dot{v} - m_{nes}(\Omega^2 u + \Omega^2 v - \ddot{u} - \ddot{v})\delta(d - r + r_i) = F\cos(\phi + t\omega)\,\delta(l - r + r_i) \quad (12)$$

$$\left(m_{nes}\ddot{u} + m_{nes}\ddot{v} - \Omega^2 m_{nes}u + k_{nes,1}u + k_{nes,2}u^3 - \Omega^2 m_{nes}v + c_{nes}\dot{u}\right)\delta(d - r + r_i) = 0 \quad (13)$$

It is obvious that the rotating beam is a clamped-free beam. Here u(t) and ν (r, t) are displacements of the NES relative to beam and displacements of the rotating beam, respectively. m, $k_{nes,1}$, $k_{nes,2}$ and c_nes are the mass, linear stiffness, nonlinearizable stiffness and damping of the NES, respectively. d represents the distance of position of connecting of the NES to beam from the base of the beam. ρ, A, l, r_i and r_o are the mass density, cross sectional area, length, inner radius and outer radius of the rotating beam, respectively. Ω is an angular velocity of the rotating beam. F and ω are amplitude and angular frequency of the external force.

The following dimensionless parameters are defined for dimensionalize of equation as:

$$\begin{aligned}
&\beta_1 = \frac{\rho A l^4 k_{nes,1}}{m_{nes}EI}, && \bar{v} = \frac{v}{l},\\
&\beta_2 = \frac{\rho A l^2 k_{nes,2}}{m_{nes}EI}, && \bar{r} = \frac{r}{l},\\
&\alpha = \frac{c_{nes}l^2}{m\sqrt{\frac{\rho A}{EI}}} && \bar{t} = \frac{t}{z},\\
&\bar{F} = \frac{\rho A l^5 F}{mEI}, && \bar{\Omega} = \Omega z,\\
&\gamma = c_b l^2\sqrt{\frac{1}{EI\rho A}}, && \bar{r}_o = \frac{r_o}{l},\\
&\eta = \left(\frac{3m_{nes}}{2l^3 I\rho A}\right), && \bar{r}_i = \frac{r_i}{l},\\
&z = \sqrt{\frac{\rho A l^4}{EI}} && \bar{u} = \frac{u}{l},\\
& && \bar{d} = \frac{d}{l},\\
& && \varepsilon = \frac{m_{nes}}{\rho A l},\\
& && \bar{\omega} = \omega z,
\end{aligned} \quad (14)$$

Employing these dimensionless parameters, the ensuing dimensionless equations of motion can be derived as follows:

$$\ddot{\bar{v}} - \bar{\Omega}^2\bar{v} + \frac{1}{2}\bar{\Omega}^2\left(2\bar{r}\bar{v}' + (\bar{r}^2 - \bar{r}_o^{\,2})\bar{v}''\right) - \varepsilon\eta{\bar{v}'}^2\bar{v}'' + \bar{v}'''' + \gamma\dot{\bar{v}} - \varepsilon(\bar{\Omega}^2\bar{u} + \bar{\Omega}^2\bar{v} - \ddot{\bar{u}} - \ddot{\bar{v}})\delta\left(\bar{d} - \bar{r} + \bar{r}_i\right) = \varepsilon\bar{F}\cos(\phi + \bar{t}\bar{\omega})\,\delta\left(\bar{l} - \bar{r} + \bar{r}_i\right) \quad (15)$$

$$(\varepsilon\ddot{\bar{u}} + \varepsilon\ddot{\bar{v}} - \bar{\Omega}^2\varepsilon\bar{u} + \varepsilon\beta_1\bar{u} + \varepsilon\beta_2\bar{u}^3 - \bar{\Omega}^2\varepsilon\bar{v} + \varepsilon\alpha\dot{\bar{u}})\delta\left(\bar{d} - \bar{r} + \bar{r}_i\right) = 0 \quad (16)$$

Using the Galerkin method, an approximate solution of the rotating beam displacement is supposed to be as:

$$v(r,t) = \sum_{j=1}^{n}\phi_j(r)q_j(r) \quad (17)$$

where ϕ_j (r) is the linear mode shape of the undamped rotating beam. Since, the rotating beam is clamped-free, the linear mode shape of the clamped-free beam is used [17]. Using the first mode of the cantilever beam ϕ_1 (r) in the Galerkin method, the following coupled equations of the NES and first mode of the rotating beam are obtained as:

$$m_b\ddot{q} + \varepsilon\phi_d^2\ddot{q} + \varepsilon\phi_d\ddot{\bar{u}} + k_b q - \varepsilon\bar{\Omega}^2\phi_d^2 q - \eta\varepsilon\lambda q^3 + \varepsilon\bar{\Omega}^2\phi_d\bar{u} + \gamma m_b\dot{q} = \bar{F}\varepsilon\cos(\phi + \bar{t}\bar{\omega})\,\phi_o \quad (18)$$

$$\varepsilon\ddot{\bar{u}} + \varepsilon\phi_d\ddot{q} + \alpha\varepsilon\dot{\bar{u}} + \varepsilon\beta_1\bar{u} - \varepsilon\bar{\Omega}^2\bar{u} - \varepsilon\bar{\Omega}^2\phi_d q + \varepsilon\beta_2\bar{u}^3 = 0 \quad (19)$$

Where m_b, k_b, λ, ϕ_o and ϕ_d are presented as:

$$m_b = \int_{\bar{r}_i}^{\bar{r}_i+1}{\phi_1}^2(\bar{r})\,d\bar{r} \quad (20)$$

$$k_b = \int_{\bar{r}_i}^{\bar{r}_i+1}\left(-\bar{\Omega}^2{\phi_1}^2(\bar{r}) + \bar{\Omega}^2\bar{r}\phi_1(\bar{r})\frac{d\phi_1(\bar{r})}{d\bar{r}} - \phi_1(\bar{r})\frac{\bar{\Omega}^2}{2}({\bar{r}^2}_o - \bar{r}^2) + \phi_1(\bar{r})\frac{d^4\phi_1(\bar{r})}{d\bar{r}^4}\right)d\bar{r} \quad (21)$$

$$\lambda = \int_{\bar{r}_i}^{\bar{r}_i+1}\left(\frac{d\phi_1(\bar{r})}{d\bar{r}}\right)^2\frac{d^2\phi_1(\bar{r})}{d\bar{r}^2}d\bar{r} \quad (22)$$

$$\phi_1(1 + \bar{r}_i) = \phi_o \quad (23)$$

$$\phi_1\left(\bar{d} + \bar{r}_i\right) = \phi_d \quad (24)$$

3- *Analytical solution*

Analytical examination of the dynamic properties of the steady-state reactions between the beam and the NES system is conducted using the Complexification-Averaging method [14-15]. To study the system's behavior near the 1:1 resonance of the first natural frequency of the rotating beam $\left(\omega_1 = \sqrt{\frac{k_{11}}{m_{11}}}\right)$, we adopt the assumption that $({\omega_1}^2 = \bar{\omega}^2 + \varepsilon\sigma)$. Consequently, we derive the following motion equations:

$$\begin{aligned} m_b\ddot{q} + \varepsilon\phi_d^2\ddot{q} + \varepsilon\phi_d\ddot{\bar{u}} + (\varepsilon\sigma + \bar{\omega}^2)m_b q \\ - \varepsilon\bar{\Omega}^2\phi_d^2 q - \eta\varepsilon\lambda q^3 \\ + \varepsilon\bar{\Omega}^2\phi_d\bar{u} + \gamma m_b\dot{q} \\ = \bar{F}\varepsilon\, cos(\phi + \bar{t}\bar{\omega})\,\phi_o \end{aligned} \tag{25}$$

$$\begin{aligned} \varepsilon\ddot{\bar{u}} + \varepsilon\phi_d\ddot{q} + \alpha\varepsilon\dot{\bar{u}} + \varepsilon\beta_1\bar{u} - \varepsilon\bar{\Omega}^2\bar{u} - \varepsilon\bar{\Omega}^2\phi_d q \\ + \varepsilon\beta_2\bar{u}^3 = 0 \end{aligned} \tag{26}$$

According to the Complexification Averaging method, the following complex parameters are introduced as:

$$e^{i\bar{t}\bar{\omega}}\varphi_1 = i\bar{\omega}u + \dot{u} \tag{27}$$

$$e^{i\bar{t}\bar{\omega}}\varphi_2 = i\bar{\omega}q + \dot{q} \tag{28}$$

Here $(e^{i\bar{t}\bar{\omega}})$ shows the fast-varying part of the dynamic of the system (the vibration frequency), and $\varphi_k, k = 1{,}2$ indicates the slow-varying, complex valued amplitude modulations. The ordinary differential equations of the slow motion are governed by:

$$\begin{aligned} \varepsilon\phi_d\dot{\varphi}_1 + \left(1 + \varepsilon\phi_d^2\right)\dot{\varphi}_2 \\ + \frac{1}{8\bar{\omega}^3}i\Big(3\varepsilon\eta\lambda{\varphi_2}^*{\varphi_2}^2 \\ + 4i\bar{\omega}^3(\varepsilon\bar{F}\phi_o - \gamma\varphi_2) \\ + 4\varepsilon\bar{\omega}^4\phi_d(\varphi_1 + \phi_d\varphi_2) \\ + 4\varepsilon\bar{\omega}^2\Big(-\sigma\varphi_2 \\ + \bar{\Omega}^2\phi_d(\varphi_1 + \phi_d\varphi_2)\Big)\Big) \\ = 0 \end{aligned} \tag{29}$$

$$\begin{aligned} \varepsilon\dot{\varphi}_1 + \varepsilon\phi_d\dot{\varphi}_2 + \frac{1}{8\bar{\omega}^3}\varepsilon\Big(4\alpha\bar{\omega}^3\varphi_1 \\ - 3i{\varphi_1}^*\beta_2{\varphi_1}^2 \\ + 4i\bar{\omega}^4(\varphi_1 + \phi_d\varphi_2) \\ + 4i\bar{\omega}^2\Big(-\beta_1\varphi_1 \\ + \bar{\Omega}^2(\varphi_1 + \phi_d\varphi_2)\Big)\Big) = 0 \end{aligned} \tag{30}$$

To find the fixed points; we equate the time derivatives of Eq. (29-30) to zero $(\dot{\varphi}_1 = 0, \dot{\varphi}_2 = 0)$ thus obtaining the following complex algebraic relations for fixed points as:

$$\begin{aligned} \frac{1}{8\bar{\omega}^3}i\Big(3\varepsilon\eta\lambda{\varphi_2}^*{\varphi_2}^2 + 4i\bar{\omega}^3(\varepsilon\bar{F}\phi_o - \gamma\varphi_2) \\ + 4\varepsilon\bar{\omega}^4\phi_d(\varphi_1 + \phi_d\varphi_2) \\ + 4\varepsilon\bar{\omega}^2\Big(-\sigma\varphi_2 \\ + \bar{\Omega}^2\phi_d(\varphi_1 + \phi_d\varphi_2)\Big)\Big) \\ = 0 \end{aligned} \tag{31}$$

$$\begin{aligned} \frac{1}{8\bar{\omega}^3}\varepsilon\Big(4\alpha\bar{\omega}^3\varphi_1 - 3i{\varphi_1}^*\beta_2{\varphi_1}^2 \\ + 4i\bar{\omega}^4(\varphi_1 + \phi_d\varphi_2) \\ + 4i\bar{\omega}^2\Big(-\beta_1\varphi_1 \\ + \bar{\Omega}^2(\varphi_1 + \phi_d\varphi_2)\Big)\Big) = 0 \end{aligned} \tag{32}$$

By simple algebraic manipulations, system Eq. (31-32) may be reduced to the following more convenient form:

$$\begin{aligned} \alpha_0 + Z\alpha_1 + Z^2\alpha_2 + Z^3\alpha_3 + Z^4\alpha_4 + Z^5\alpha_5 \\ + Z^6\alpha_6 + Z^7\alpha_7 + Z^8\alpha_8 \\ + Z^9\alpha_9 = 0 \end{aligned} \tag{33}$$

$$|\phi_{10}|^2 = Z \tag{34}$$

The coefficients of equation Eq. (33-34) are presented in Appendix A.

Eq. (33-34) may yield one or more responses based on the values of its parameters. Furthermore, it shows that the system's response is continuous, leading to several bifurcation points, such as saddle-node and Hopf bifurcations, within the system's response. To identify saddle-node bifurcations, the derivatives of Eq. (33) must be zero [27].

$$\begin{aligned} \alpha_1 + 2Z\alpha_2 + 3Z^2\alpha_3 + 4Z^3\alpha_4 + 5Z^4\alpha_5 \\ + 6Z^5\alpha_6 + 7Z^6\alpha_7 + 8Z^7\alpha_8 \\ + 9Z^8\alpha_9 = 0 \end{aligned} \tag{35}$$

Additionally, the existence conditions for the Hopf bifurcation are determined by introducing small complex perturbation terms, $\delta_1(\bar{t})$ and $\delta_2(\bar{t})$, around the equilibrium points. The slow-varying modulation is reintroduced as

$$\varphi_2(\bar{t}) = \varphi_{20} + \delta_2(\bar{t}) \tag{36}$$

$$\varphi_1(\bar{t}) = \varphi_{10} + \delta_1(\bar{t}) \tag{37}$$

By substituting Eq. (36-37) into Eq. (29-30) and neglecting the nonlinear perturbation terms, we derive four coupled ordinary differential equations near the equilibrium point.

$$\dot{\delta}_1 = \phi_d\left(\frac{3i{\delta_1}^*\beta_2(1+\varepsilon\phi_d^2)\varphi_{10}^2}{8\bar{\omega}^3\phi_d} + \frac{3i\varepsilon\eta\lambda{\delta_2}^*\varphi_{20}^2}{8\bar{\omega}^3} + \left(-\frac{i\left(2\bar{\omega}^4 - 2i\bar{\omega}^3(\alpha+\alpha\varepsilon\phi_d^2) + 2\bar{\omega}^2\left(\bar{\Omega}^2 - \beta_1(1+\varepsilon\phi_d^2)\right) - 3{\varphi_{10}}^*\beta_2(1+\varepsilon\phi_d^2)\varphi_{10}\right)}{4\bar{\omega}^3\phi_d}\right)\delta_1 - \left(\frac{i(2i\gamma\bar{\omega}^3 + 2\bar{\omega}^4 + 2\bar{\omega}^2(\varepsilon\sigma+\bar{\Omega}^2) - 3\varepsilon\eta\lambda{\varphi_{20}}^*\varphi_{20})}{4\bar{\omega}^3}\right)\delta_2\right) \tag{38}$$

$$\dot{\delta}_2 = -\frac{1}{\varepsilon\phi_d}\left(\frac{3i\varepsilon^2{\delta_1}^*\beta_2\phi_d^2\varphi_{10}^2}{8\bar{\omega}^3} + \frac{3i\varepsilon^2\eta\lambda{\delta_2}^*\phi_d\varphi_{20}^2}{8\bar{\omega}^3} + \left(\frac{\varepsilon^2\phi_d^2(-2\alpha\bar{\omega}^3 + 2i\bar{\omega}^2\beta_1 + 3i{\varphi_{10}}^*\beta_2\varphi_{10})}{4\bar{\omega}^3}\right)\delta_1 + \left(\frac{\varepsilon\phi_d(-2i\varepsilon\sigma\bar{\omega}^2 + 2\gamma\bar{\omega}^3 + 3i\varepsilon\eta\lambda{\varphi_{20}}^*\varphi_{20})}{4\bar{\omega}^3}\right)\delta_2\right) \tag{39}$$

$${\dot{\delta}_1}^* = \phi_d\left(\frac{1}{4\bar{\omega}^3\phi_d}i{\delta_1}^*\left(2\bar{\omega}^4 + 2i\bar{\omega}^3(\alpha+\alpha\varepsilon\phi_d^2) + 2\bar{\omega}^2\left(\bar{\Omega}^2 - \beta_1(1+\varepsilon\phi_d^2)\right) - 3{\varphi_{10}}^*\beta_2(1+\varepsilon\phi_d^2)\varphi_{10}\right) + \frac{1}{4}{\delta_2}^*\left(2\gamma + 2i\bar{\omega} + \frac{2i(\varepsilon\sigma+\bar{\Omega}^2)}{\bar{\omega}} - \frac{3i\varepsilon\eta\lambda{\varphi_{20}}^*\varphi_{20}}{\bar{\omega}^3}\right) - \left(\frac{3i{\varphi_{10}}^{*2}\beta_2(1+\varepsilon\phi_d^2)}{8\bar{\omega}^3\phi_d}\right)\delta_1 - \left(\frac{3i\varepsilon\eta\lambda{\varphi_{20}}^{*2}}{8\bar{\omega}^3}\right)\delta_2\right) \tag{40}$$

$${\dot{\delta}_2}^* = \frac{1}{\varepsilon\phi_d}\left(+\frac{\varepsilon^2\phi_d^2(2\alpha\bar{\omega}^3 + 2i\bar{\omega}^2\beta_1 + 3i{\varphi_{10}}^*\beta_2\varphi_{10})}{4\bar{\omega}^3}{\delta_1}^* - \frac{\varepsilon\phi_d(2i\varepsilon\sigma\bar{\omega}^2 + 2\gamma\bar{\omega}^3 - 3i\varepsilon\eta\lambda{\varphi_{20}}^*\varphi_{20})}{4\bar{\omega}^3}{\delta_2}^* + \left(\frac{3i\varepsilon^2{\varphi_{10}}^{*2}\beta_2\phi_d^2}{8\bar{\omega}^3}\right)\delta_1 + \left(\frac{3i\varepsilon^2\eta\lambda{\varphi_{20}}^{*2}\phi_d}{8\bar{\omega}^3}\right)\delta_2\right) \tag{41}$$

The stars in Eq. (38-41) denote the complex conjugates of the respective parameters. The characteristic polynomial of these four coupled equations is

$$\chi^4 + \chi^3\nu_4 + \chi^2\nu_3 + \chi(\nu_2 + i\nu_5) + \nu_1 = 0 \tag{42}$$

The coefficients of Eq. (42) are detailed in Appendix B. A Hopf bifurcation occurs when the characteristic polynomial yields a pair of purely complex conjugate roots as $\chi = \pm i\Omega'$. In fact, Ω' represents the characteristic frequency of the periodic orbits emerging from the bifurcation of the fixed points. Inserting this relationship into Eq. (42) and isolating the real and imaginary components of the equation results in

$$\nu_2^4 - 2\nu_2^3\nu_3\nu_4 + \nu_2^2(2\nu_1 + \nu_3^2)\nu_4^2 + \nu_1^2\nu_4^4 - \nu_2\nu_4^3(2\nu_1\nu_3 + \nu_5^2) = 0 \tag{43}$$

Eq. (26) outlines the essential conditions required for the occurrence of a Hopf bifurcation. It provides the mathematical prerequisites that must be satisfied for this type of bifurcation to take place, highlighting the specific criteria that indicate the transition to a new behavior within the system dynamics.

4- *Results and Disscution*

In this study, the frequency response curves of the system under varying parameters are analyzed and presented in Figures 2 through 12. The response is evaluated by altering the excitation amplitude F, the linear stiffness coefficient β_1, the nonlinear stiffness coefficient β_2 , the NES damping coefficient α, the beam nonlinear coefficient η, and the beam damping coefficient γ. The dimensionless frequency detuning parameter σ is plotted against the amplitude on a logarithmic scale, illustrating the system's dynamic behavior across a wide range of conditions.

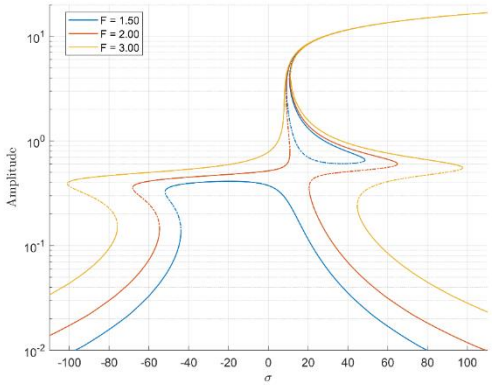

Fig. 2) The Frequency response curves of the system for various external amplitude

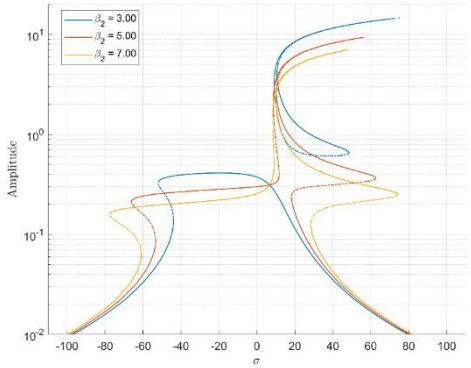

Fig. 3) The Frequency response curves of the system for various dimensionless stiffness coefficient with F=1.5

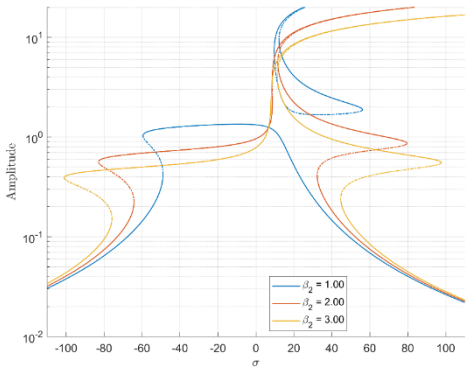

Fig. 4) The Frequency response curves of the system for various dimensionless stiffness coefficient with F=3

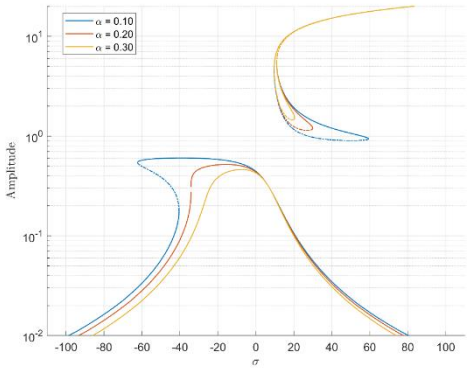

Fig. 5) The Frequency response curves of the system for various dimensionless NES damping coefficient with F=1.5

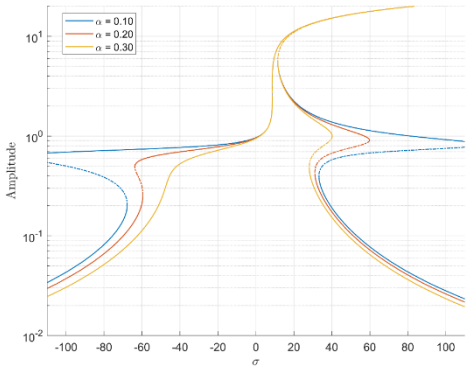

Fig. 6) The Frequency response curves of the system for various dimensionless NES damping coefficient with F=3

In (Ref. to figure 2), frequency response curves of the system are plotted for excitation amplitudes F=1.50, 2.00, 3.00. As F increases, the peak amplitude also increases, and the resonance curves shift to higher frequencies. This shift is accompanied by broader resonance peaks, indicating more significant nonlinear behavior at higher excitation levels. And it can be seen that in higher excitation amplitude the higher-amplitude island-like region in the curves and the lower amplitude zone of curves are connected to each other. The multivalued regions, representing multiple stable and unstable solutions, expand as the excitation amplitude increases.

(Ref. to figure 3) examines the influence of the nonlinear stiffness coefficient β_2 with values $\beta_2 = 3.00,\ 5.00,\ 7.00$. Increasing β_2 leads to a reduction in amplitude at the resonance. A similar trend is observed in (Ref. to figure 4), where β_2 values of 1.00, 2.00, and 3.00 are considered. The amplitude decreases more noticeably at lower β_2 values, with the response curves displaying more significant changes. This behavior, indicative of nonlinear dynamics, could potentially be explained by bifurcation theory or other aspects of nonlinear oscillations

The effects of varying the NES damping coefficient α are shown in (Ref. to figure 5) for α= 0.10, 0.20, 0.30. Higher α values result reduction of hand-like parts. This damping effect suppresses the system's nonlinear characteristics, reducing the size of the multivalued regions. These observations are consistent in (Ref. to figure 6), where further increases in α lead to additional attenuation of the system's response, further smoothing out the resonance behavior.

The influence of the linear stiffness coefficient β_1 is depicted in (Ref. to figure 7), where β_1 is varied between 0.80, 1.10, and 1.70. Increasing β_1 suppresses the system's nonlinear characteristics, reducing the size of the multivalued regions. This issue reduces nonlinear effects in the system and the system becomes linear. This trend is also observed in (Ref. to figure 8), with higher β_1 values resulting reducing the size of the multivalued regions.

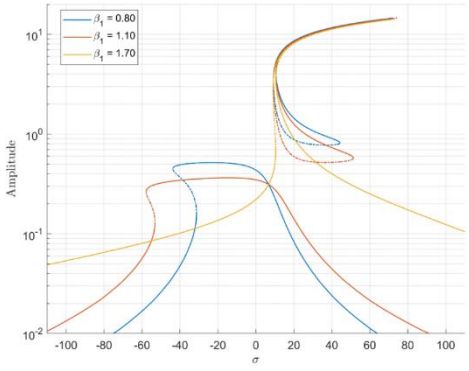

Fig. 7) The Frequency response curves of the system for various dimensionless NES linear stiffness coefficient with F=1.5

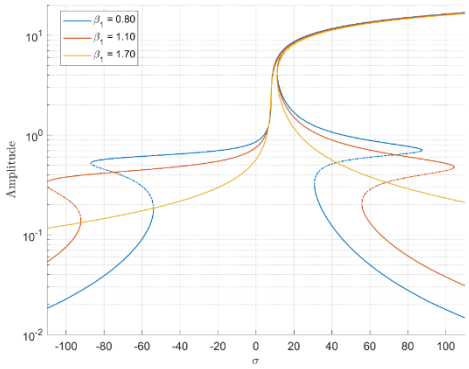

Fig. 8) The Frequency response curves of the system for various dimensionless NES linear stiffness coefficient with F=3

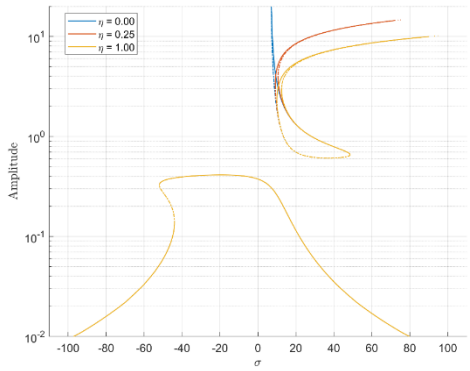

Fig. 9) The Frequency response curves of the system for various beam nonlinear coefficient with F=1.5

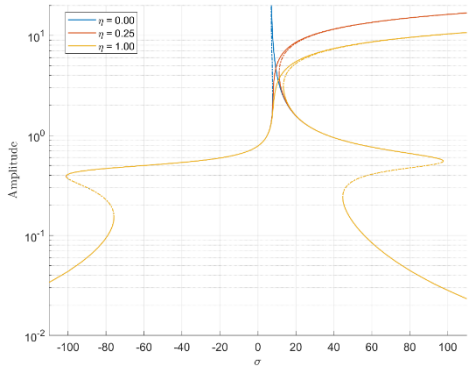

Fig. 10) The Frequency response curves of the system for various beam nonlinear coefficient with F=3

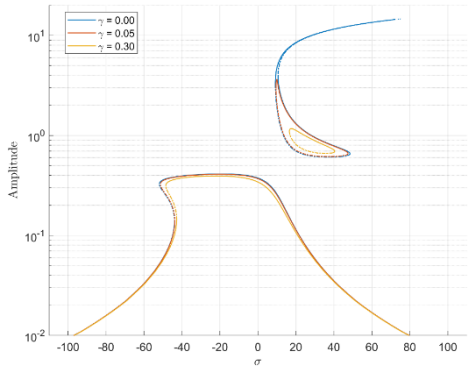

Fig. 11) The Frequency response curves of the system for various beam damping coefficient

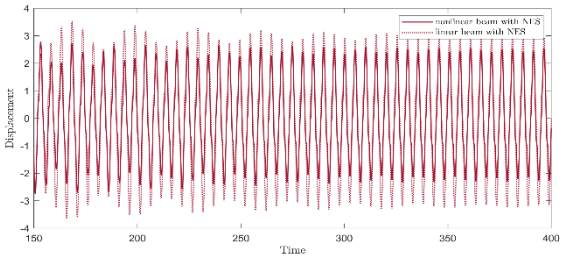

Fig. 12) The Frequency response curves of the system for various dimensionless NES linear stiffness coefficient with F=3

The beam nonlinear coefficient η is varied in (Ref. to figure 9) with values $\eta = 0,\ 0.25,\ 1.00$. As η increases, the curves exhibit Hardening behavior, especially for higher η values. This indicates that the beam's nonlinear characteristics significantly influence the system's dynamic behavior. In (Ref. to figure 10), these effects are further illustrated, where increasing η leads to the emergence of Hardening behavior, suggesting complex dynamic interactions within the system.
The impact of the beam damping coefficient γ is illustrated in (Ref. to figure 11). Increasing γ values (0.00, 0.05, 0.30) lead to a reduction in the overall amplitude and a narrowing of the resonance peaks.
Finaly, by studying the time response of linear and nonlinear systems, difference of system behavior in two cases resulting from the nonlinearity of the beam and its effect which reduces the vibration amplitude is observable (Ref. to figure 12).

5- *Conclusion*

This study has examined the effects of various system parameters on the vibration of a nonlinear rotating beam subjected to external forces, focusing on vibration reduction through a nonlinear energy sink (NES) positioned at the beam's center. The beam was modeled using the Euler-Bernoulli beam theory and von Kármán strain-displacement relations, with the equations of motion derived via Hamilton's principle. The analysis indicates that increasing the force amplitude or spring coefficient shifts the high-frequency island-like regions in the response curves towards lower frequencies, a phenomenon consistent with nonlinear dynamic behavior, potentially explained by bifurcation theory. The study identifies the presence of saddle-node bifurcations, marking abrupt changes in system stability, and Hopf bifurcations, leading to oscillatory behaviors. Furthermore, an increase in the spring coefficient reduces the vibration amplitude, while an increase in the nonlinear coefficient results in hardening behavior, effectively reducing the overall vibration amplitude. These findings underscore the significance of the system's nonlinearity and the NES's role in controlling its dynamic response, providing valuable insights for the design of effective vibration mitigation strategies.

Declaration of competing interest

The authors declare that they have no known competing financial interests or personal relationships that could have appeared to influence the work reported in this paper.

References

1–Bab S, Khadem SE, Mahdiabadi MK, Shahgholi M. Vibration mitigation of a rotating beam under external periodic force using a nonlinear energy sink (NES). Journal of Vibration and Control. 2017 Apr;23(6):1001-25.

2- Bera KK, Aravind G, Banerjee A. Vibration control of a pre-twisted rotating beam with nonlinear bi-stable attachments. InStructures 2023 Nov 1 (Vol. 57, p. 105050). Elsevier.

3- Abdollahi A, Khadem SE, Khazaee M, Moslemi A. On the analysis of a passive vibration absorber for submerged beams under hydrodynamic forces: An optimal design. Engineering Structures. 2020 Oct 1;220:110986.

4- Bukhari M, Barry O. Exact nonlinear dynamic analysis of a beam with a nonlinear vibration absorber and with various boundary conditions. Journal of Computational and Nonlinear Dynamics. 2020 Jan 1;15(1):011003.

5- Chouvion B. Vibration analysis of beam structures with localized nonlinearities by a wave approach. Journal of Sound and Vibration. 2019 Jan 20;439:344-61.

6- Zhao Y, Du J, Liu Y. Vibration suppression and dynamic behavior analysis of an axially loaded beam with NES and nonlinear elastic supports. Journal of Vibration and Control. 2023 Feb;29(3-4):844-57.

7- Pesheck E, Pierre C, Shaw SW. Modal reduction of a nonlinear rotating beam through nonlinear normal modes. J. Vib. Acoust.. 2002 Apr 1;124(2):229-36.

8- Baxy A, Sarkar A. Natural frequencies of rotating twisted beams: a perturbation method based approach. Meccanica. 2020 Oct;55:2075-89.

9- Huang J, Zhou K, Xu J, Wang K, Song H. Flap-wise vibrations of non-uniform rotating cantilever beams: An investigation with operational experiments. Journal of Sound and Vibration. 2023 Jun 9;553:117648.

10- Basta E, Ghommem M, Emam S. Vibration suppression of nonlinear rotating metamaterial beams. Nonlinear Dynamics. 2020 Jul;101:311-32.

11- Wu J, Titurus B. Vibration control of a rotating Timoshenko beam-tendon system via internal guiding inerter-dampers. Journal of Sound and Vibration. 2022 Jan 6;516:116542.

12- Hao S, Yamashita Y, Kobayashi K. Passivity-based control of nonlinear active dynamic vibration absorber. International Journal of Robust and Nonlinear Control. 2023 Mar 25;33(5):3247-66.

13- Zhang Z, Gao ZT, Fang B, Zhang YW. Vibration suppression of a geometrically nonlinear beam with boundary inertial nonlinear energy sinks. Nonlinear Dynamics. 2022 Aug;109(3):1259-75.

14- Samani FS, Pellicano F, Masoumi A. Performances of dynamic vibration absorbers for beams subjected to moving loads. Nonlinear Dynamics. 2013 Jul;73:1065-79.

15- Wang L, Su Z, Wang L. Inplane vibration analysis of rotating beams with elastic restraints. Journal of Vibration and Control. 2023 Apr;29(7-8):1484-97.

16- Fang Y, Li L, Zhang D, Chen S, Liao WH. Vibration suppression of a rotating functionally graded beam with enhanced active constrained layer damping treatment in temperature field. Thin-Walled Structures. 2021 Apr 1;161:107522.

17- Meirovitch L. Fundamentals of vibrations. Waveland Press; 2010 Jun 17.

18- Manevich AI, Manevich LI. The mechanics of nonlinear systems with internal resonances. World Scientific; 2005.

19- Balaji PS, Karthik SelvaKumar K. Applications of nonlinearity in passive vibration control: a review. Journal of Vibration Engineering & Technologies. 2021 Feb;9:183-213.

20- Nazari MM, Rahi A. Parameters optimization of a nonlinear dynamic absorber for a nonlinear system. Archive of Applied Mechanics. 2023 Aug;93(8):3243-58.

21- Haris A, Alevras P, Mohammadpour M, Theodossiades S, O'Mahony M. Design and validation of a nonlinear vibration absorber to attenuate torsional oscillations of propulsion systems. Nonlinear Dynamics. 2020 Mar;100:33-49.

22- Feudo SL, Touzé C, Boisson J, Cumunel G. Nonlinear magnetic vibration absorber for passive control of a multi–storey structure. Journal of Sound and Vibration. 2019 Jan 6;438:33-53.

23- Liao P. Non-linear vibration and bifurcation analysis of Euler-Bernoulli beam under parametric excitation. Journal of Engineering and Applied Science. 2024 Dec;71(1):85.

24- Younesian D, Esmailzadeh E. Vibration suppression of rotating beams using time-varying internal tensile force. Journal of sound and vibration. 2011 Jan 17;330(2):308-20.

25- Pipes LA. Analysis of a nonlinear dynamic vibration absorber.

26- de Bruin JC. Application of a dynamic vibration absorber to a piecewise linear beam system under pre-tension.

27- Nayfeh AH, Balachandran B. Applied nonlinear dynamics: analytical, computational, and experimental methods. John Wiley & Sons; 2008 Nov 20.

Appendix A

$$\alpha_0 = -\varepsilon^2\bar{F}^2\phi_o^2$$

$$\alpha_1 = \frac{1}{4\bar{\omega}^2(\bar{\omega}^2+\bar{\Omega}^2)^2\phi_d^2}(\bar{\omega}^6(\gamma+\alpha\varepsilon\phi_d^2)^2+\bar{\omega}^4(\alpha^2\gamma^2+\varepsilon^2\sigma^2-2\alpha^2\varepsilon^2\sigma\phi_d^2+\varepsilon^2\beta_1^2\phi_d^4+2\bar{\Omega}^2(\gamma+\alpha\varepsilon\phi_d^2)^2-2\beta_1(\gamma^2-\varepsilon^2\sigma\phi_d^2))+\varepsilon^2(\sigma\beta_1-\bar{\Omega}^2(\sigma+\beta_1\phi_d^2))^2+\bar{\omega}^2(\alpha^2\varepsilon^2\sigma^2-2\varepsilon^2\sigma^2\beta_1+\bar{\Omega}^4(\gamma+\alpha\varepsilon\phi_d^2)^2+\beta_1^2(\gamma^2-2\varepsilon^2\sigma\phi_d^2)+2\bar{\Omega}^2(\varepsilon^2\beta_1^2\phi_d^4+\varepsilon^2\sigma(\sigma-\alpha^2\phi_d^2)-\beta_1(\gamma^2-2\varepsilon^2\sigma\phi_d^2))))$$

$$\alpha_2 = \frac{1}{8\bar{\omega}^4(\bar{\omega}^2+\bar{\Omega}^2)^4\phi_d^4}3(\bar{\omega}^8(-\varepsilon^2\eta\lambda\sigma+(\alpha^2\varepsilon^2\eta\lambda-\varepsilon^2\eta\lambda\beta_1-\gamma^2\beta_2)\phi_d^2+\varepsilon^2\sigma\beta_2\phi_d^4+\varepsilon^2\beta_1\beta_2\phi_d^6)-\varepsilon^2(-\sigma\beta_1+\bar{\Omega}^2(\sigma+\beta_1\phi_d^2))(3\eta\lambda\bar{\Omega}^2\beta_1^2-\eta\lambda\beta_1^3+\bar{\Omega}^4(-3\eta\lambda\beta_1+\sigma\beta_2\phi_d^2)+\bar{\Omega}^6(\eta\lambda-\beta_2\phi_d^4))+\bar{\omega}^6(3\varepsilon^2\eta\lambda\beta_1^2\phi_d^2+\varepsilon^2(-2\alpha^2\eta\lambda\sigma+(\alpha^4\eta\lambda-\sigma^2\beta_2)\phi_d^2)+\beta_1(4\varepsilon^2\eta\lambda\sigma+(-3\alpha^2\varepsilon^2\eta\lambda+\gamma^2\beta_2)\phi_d^2-2\varepsilon^2\sigma\beta_2\phi_d^4)+\bar{\Omega}^2(-4\varepsilon^2\eta\lambda\sigma+(3\alpha^2\varepsilon^2\eta\lambda-4\varepsilon^2\eta\lambda\beta_1-3\gamma^2\beta_2)\phi_d^2+4\varepsilon^2\sigma\beta_2\phi_d^4+4\varepsilon^2\beta_1\beta_2\phi_d^6))+\bar{\omega}^2(\varepsilon^2\eta\lambda\beta_1^2(-2\alpha^2\sigma+4\sigma\beta_1+\beta_1^2\phi_d^2)+\bar{\Omega}^6(-4\varepsilon^2\eta\lambda\sigma+(\alpha^2\varepsilon^2\eta\lambda-4\varepsilon^2\eta\lambda\beta_1-\gamma^2\beta_2)\phi_d^2+4\varepsilon^2\sigma\beta_2\phi_d^4+4\varepsilon^2\beta_1\beta_2\phi_d^6)+2\varepsilon^2\bar{\Omega}^2\beta_1(-3\eta\lambda\beta_1^2\phi_d^2+\eta\lambda\beta_1(-6\sigma+\alpha^2\phi_d^2)+\sigma(2\alpha^2\eta\lambda+\sigma\beta_2\phi_d^2))+\bar{\Omega}^4(9\varepsilon^2\eta\lambda\beta_1^2\phi_d^2-\varepsilon^2\sigma(2\alpha^2\eta\lambda+3\sigma\beta_2\phi_d^2)+\beta_1(12\varepsilon^2\eta\lambda\sigma+(-3\alpha^2\varepsilon^2\eta\lambda+\gamma^2\beta_2)\phi_d^2-6\varepsilon^2\sigma\beta_2\phi_d^4)))+\bar{\omega}^4(\bar{\Omega}^4(-6\varepsilon^2\eta\lambda\sigma+3(\alpha^2\varepsilon^2\eta\lambda-2\varepsilon^2\eta\lambda\beta_1-\gamma^2\beta_2)\phi_d^2+6\varepsilon^2\sigma\beta_2\phi_d^4+6\varepsilon^2\beta_1\beta_2\phi_d^6)+\varepsilon^2(-\alpha^4\eta\lambda\sigma-3\eta\lambda\beta_1^3\phi_d^2+2\eta\lambda\beta_1^2(-3\sigma+\alpha^2\phi_d^2)+\sigma\beta_1(4\alpha^2\eta\lambda+\sigma\beta_2\phi_d^2))+\bar{\Omega}^2(9\varepsilon^2\eta\lambda\beta_1^2\phi_d^2+\varepsilon^2(-4\alpha^2\eta\lambda\sigma+(\alpha^4\eta\lambda-3\sigma^2\beta_2)\phi_d^2)+2\beta_1(6\varepsilon^2\eta\lambda\sigma+(-3\alpha^2\varepsilon^2\eta\lambda+\gamma^2\beta_2)\phi_d^2-3\varepsilon^2\sigma\beta_2\phi_d^4))))$$

$$\alpha_3 = \frac{1}{64\bar{\omega}^6(\bar{\omega}^2+\bar{\Omega}^2)^6\phi_d^6}9(\varepsilon^2\bar{\omega}^{12}(\eta\lambda-\beta_2\phi_d^4)^2+\bar{\omega}^{10}(3\alpha^2\varepsilon^2\eta^2\lambda^2+8\varepsilon^2\eta\lambda\sigma\beta_2\phi_d^2-6\alpha^2\varepsilon^2\eta\lambda\beta_2\phi_d^4+\gamma^2\beta_2^2\phi_d^4-2\varepsilon^2\sigma\beta_2^2\phi_d^6-6\varepsilon^2\eta\lambda\beta_1(\eta\lambda-2\beta_2\phi_d^4)+6\varepsilon^2\bar{\Omega}^2(\eta\lambda-\beta_2\phi_d^4)^2)+\varepsilon^2(-6\eta^2\lambda^2\bar{\Omega}^2\beta_1^5+\eta^2\lambda^2\beta_1^6+\eta\lambda\bar{\Omega}^4\beta_1^3(15\eta\lambda\beta_1-8\sigma\beta_2\phi_d^2)+\bar{\Omega}^{12}(\eta\lambda-\beta_2\phi_d^4)^2+\bar{\Omega}^8(-24\eta\lambda\sigma\beta_1\beta_2\phi_d^2+\sigma^2\beta_2^2\phi_d^4+3\eta\lambda\beta_1^2(5\eta\lambda-6\beta_2\phi_d^4))-2\bar{\Omega}^{10}(3\eta\lambda\beta_1(\eta\lambda-2\beta_2\phi_d^4)+\sigma\beta_2\phi_d^2(-4\eta\lambda+\beta_2\phi_d^4))+4\eta\lambda\bar{\Omega}^6\beta_1^2(6\sigma\beta_2\phi_d^2+\beta_1(-5\eta\lambda+2\beta_2\phi_d^4)))+\bar{\omega}^8(15\varepsilon^2\bar{\Omega}^4(\eta\lambda-\beta_2\phi_d^4)^2+2\bar{\Omega}^2(6\alpha^2\varepsilon^2\eta^2\lambda^2+4\varepsilon^2\eta\lambda\beta_2\phi_d^2(5\sigma-3\alpha^2\phi_d^2)-15\varepsilon^2\eta\lambda\beta_1(\eta\lambda-2\beta_2\phi_d^4)+\beta_2^2(2\gamma^2\phi_d^4-5\varepsilon^2\sigma\phi_d^6))+\varepsilon^2(3\alpha^4\eta^2\lambda^2+8\alpha^2\eta\lambda\sigma\beta_2\phi_d^2+\sigma^2\beta_2^2\phi_d^4+3\eta\lambda\beta_1^2(5\eta\lambda-6\beta_2\phi_d^4)-4\eta\lambda\beta_1(3\alpha^2\eta\lambda+\beta_2(6\sigma\phi_d^2-2\alpha^2\phi_d^4))))+\bar{\omega}^6(20\varepsilon^2\bar{\Omega}^6(\eta\lambda-\beta_2\phi_d^4)^2+\varepsilon^2\eta\lambda(\alpha^6\eta\lambda+6\beta_1^2(3\alpha^2\eta\lambda+4\sigma\beta_2\phi_d^2)-2\beta_1(3\alpha^4\eta\lambda+4\alpha^2\sigma\beta_2\phi_d^2)+\beta_1^3(-20\eta\lambda+8\beta_2\phi_d^4))+2\bar{\Omega}^4(9\alpha^2\varepsilon^2\eta^2\lambda^2+2\varepsilon^2\eta\lambda\beta_2\phi_d^2(20\sigma-9\alpha^2\phi_d^2)-30\varepsilon^2\eta\lambda\beta_1(\eta\lambda-2\beta_2\phi_d^4)+\beta_2^2(3\gamma^2\phi_d^4-10\varepsilon^2\sigma\phi_d^6))+2\varepsilon^2\bar{\Omega}^2(3\alpha^4\eta^2\lambda^2+12\alpha^2\eta\lambda\sigma\beta_2\phi_d^2+2\sigma^2\beta_2^2\phi_d^4+6\eta\lambda\beta_1^2(5\eta\lambda-6\beta_2\phi_d^4)-6\eta\lambda\beta_1(3\alpha^2\eta\lambda+\beta_2(8\sigma\phi_d^2-2\alpha^2\phi_d^4))))+\bar{\omega}^4(15\varepsilon^2\bar{\Omega}^8(\eta\lambda-\beta_2\phi_d^4)^2+\varepsilon^2\eta\lambda\beta_1^2(3\alpha^4\eta\lambda+15\eta\lambda\beta_1^2-4\beta_1(3\alpha^2\eta\lambda+2\sigma\beta_2\phi_d^2))+4\bar{\Omega}^6(3\alpha^2\varepsilon^2\eta^2\lambda^2+2\varepsilon^2\eta\lambda\beta_2\phi_d^2(10\sigma-3\alpha^2\phi_d^2)+\beta_2^2\phi_d^4(\gamma^2-5\varepsilon^2\sigma\phi_d^2)-15\varepsilon^2\eta\lambda\beta_1(\eta\lambda-2\beta_2\phi_d^4))+2\varepsilon^2\eta\lambda\bar{\Omega}^2\beta_1(-3\alpha^4\eta\lambda-8\alpha^2\sigma\beta_2\phi_d^2+18\beta_1(\alpha^2\eta\lambda+2\sigma\beta_2\phi_d^2)-6\beta_1^2(5\eta\lambda-2\beta_2\phi_d^4))+3\varepsilon^2\bar{\Omega}^4(\alpha^4\eta^2\lambda^2+8\alpha^2\eta\lambda\sigma\beta_2\phi_d^2+2\sigma^2\beta_2^2\phi_d^4+6\eta\lambda\beta_1^2(5\eta\lambda-6\beta_2\phi_d^4)-4\eta\lambda\beta_1(3\alpha^2\eta\lambda+2\beta_2(6\sigma\phi_d^2-\alpha^2\phi_d^4))))+\bar{\omega}^2(3\varepsilon^2\eta^2\lambda^2(\alpha^2-2\beta_1)\beta_1^4+2\varepsilon^2\eta\lambda\bar{\Omega}^2\beta_1^3(-6\alpha^2\eta\lambda+15\eta\lambda\beta_1-8\sigma\beta_2\phi_d^2)+6\varepsilon^2\bar{\Omega}^{10}(\eta\lambda-\beta_2\phi_d^4)^2+\bar{\Omega}^8(3\alpha^2\varepsilon^2\eta^2\lambda^2+2\varepsilon^2\eta\lambda\beta_2\phi_d^2(20\sigma-3\alpha^2\phi_d^2)+\beta_2^2\phi_d^4(\gamma^2-10\varepsilon^2\sigma\phi_d^2)-30\varepsilon^2\eta\lambda\beta_1(\eta\lambda-2\beta_2\phi_d^4))+2\varepsilon^2\eta\lambda\bar{\Omega}^4\beta_1(-4\alpha^2\sigma\beta_2\phi_d^2+9\beta_1(\alpha^2\eta\lambda+4\sigma\beta_2\phi_d^2)-6\beta_1^2(5\eta\lambda-2\beta_2\phi_d^4))+4\varepsilon^2\bar{\Omega}^6(\sigma\beta_2\phi_d^2(2\alpha^2\eta\lambda+\sigma\beta_2\phi_d^2)+3\eta\lambda\beta_1^2(5\eta\lambda-6\beta_2\phi_d^4)+\eta\lambda\beta_1(-3\alpha^2\eta\lambda+\beta_2(-24\sigma\phi_d^2+2\alpha^2\phi_d^4)))))$$

$$\alpha_4 = -\frac{1}{128\bar{\omega}^8(\bar{\omega}^2+\bar{\Omega}^2)^6\phi_d^6}27\varepsilon^2\eta\lambda\beta_2(3\bar{\omega}^{10}(\eta\lambda-\beta_2\phi_d^4)+\bar{\omega}^8(6\alpha^2\eta\lambda+6\sigma\beta_2\phi_d^2-2\alpha^2\beta_2\phi_d^4+15\bar{\Omega}^2(\eta\lambda-\beta_2\phi_d^4)+\beta_1(-15\eta\lambda+9\beta_2\phi_d^4))+3(\bar{\Omega}^2-\beta_1)(-4\eta\lambda\bar{\Omega}^2\beta_1^3+\eta\lambda\beta_1^4+2\bar{\Omega}^4\beta_1(3\eta\lambda\beta_1-\sigma\beta_2\phi_d^2)+\bar{\Omega}^8(\eta\lambda-\beta_2\phi_d^4)+2\bar{\Omega}^6(\sigma\beta_2\phi_d^2+\beta_1(-2\eta\lambda+\beta_2\phi_d^4)))+\bar{\omega}^6(3\alpha^4\eta\lambda+2\alpha^2\sigma\beta_2\phi_d^2-6\beta_1(3\alpha^2\eta\lambda+2\sigma\beta_2\phi_d^2)+30\bar{\Omega}^4(\eta\lambda-\beta_2\phi_d^4)+6\beta_1^2(5\eta\lambda-\beta_2\phi_d^4)+6\bar{\Omega}^2(3\alpha^2\eta\lambda+\beta_2(4\sigma\phi_d^2-\alpha^2\phi_d^4)+\beta_1(-10\eta\lambda+6\beta_2\phi_d^4)))+\bar{\omega}^4(30\bar{\Omega}^6(\eta\lambda-\beta_2\phi_d^4)-3\beta_1(\alpha^4\eta\lambda+10\eta\lambda\beta_1^2-2\beta_1(3\alpha^2\eta\lambda+\sigma\beta_2\phi_d^2))+\bar{\Omega}^2(3\alpha^4\eta\lambda+4\alpha^2\sigma\beta_2\phi_d^2-36\beta_1(\alpha^2\eta\lambda+\sigma\beta_2\phi_d^2)+18\beta_1^2(5\eta\lambda-\beta_2\phi_d^4))+6\bar{\Omega}^4(3\alpha^2\eta\lambda+\beta_2(6\sigma\phi_d^2-\alpha^2\phi_d^4)+\beta_1(-15\eta\lambda+9\beta_2\phi_d^4)))+\bar{\omega}^2(3\eta\lambda\beta_1^3(-2\alpha^2+5\beta_1)+6\bar{\Omega}^2\beta_1^2(3\alpha^2\eta\lambda-10\eta\lambda\beta_1+2\sigma\beta_2\phi_d^2)+15\bar{\Omega}^8(\eta\lambda-\beta_2\phi_d^4)-2\bar{\Omega}^4(-\alpha^2\sigma\beta_2\phi_d^2+9\beta_1(\alpha^2\eta\lambda+2\sigma\beta_2\phi_d^2)+\beta_1^2(-45\eta\lambda+9\beta_2\phi_d^4))+\bar{\Omega}^6(6\alpha^2\eta\lambda+\beta_2(24\sigma\phi_d^2-2\alpha^2\phi_d^4)+\beta_1(-60\eta\lambda+36\beta_2\phi_d^4))))$$

$$\alpha_5 = \frac{1}{1024\bar{\omega}^{10}(\bar{\omega}^2+\bar{\Omega}^2)^6\phi_d^6}81\varepsilon^2\eta\lambda\beta_2^2(-60\eta\lambda\bar{\Omega}^2\beta_1^3+15\eta\lambda\beta_1^4+2\bar{\Omega}^4\beta_1(45\eta\lambda\beta_1-4\sigma\beta_2\phi_d^2)+3\bar{\omega}^8(5\eta\lambda-2\beta_2\phi_d^4)+3\bar{\Omega}^8(5\eta\lambda-2\beta_2\phi_d^4)+2\bar{\omega}^6(9\alpha^2\eta\lambda+4\sigma\beta_2\phi_d^2+6\bar{\Omega}^2(5\eta\lambda-2\beta_2\phi_d^4)+\beta_1(-30\eta\lambda+4\beta_2\phi_d^4))+\bar{\Omega}^6(8\sigma\beta_2\phi_d^2+\beta_1(-60\eta\lambda+8\beta_2\phi_d^4))+\bar{\omega}^4(3\alpha^4\eta\lambda+90\eta\lambda\beta_1^2-4\beta_1(9\alpha^2\eta\lambda+2\sigma\beta_2\phi_d^2)+18\bar{\Omega}^4(5\eta\lambda-2\beta_2\phi_d^4)+12\bar{\Omega}^2(3\alpha^2\eta\lambda+2\sigma\beta_2\phi_d^2+\beta_1(-15\eta\lambda+2\beta_2\phi_d^4)))+2\bar{\omega}^2(3\eta\lambda(3\alpha^2-10\beta_1)\beta_1^2+2\bar{\Omega}^2\beta_1(-9\alpha^2\eta\lambda+45\eta\lambda\beta_1-4\sigma\beta_2\phi_d^2)+6\bar{\Omega}^6(5\eta\lambda-2\beta_2\phi_d^4)+3\bar{\Omega}^4(3\alpha^2\eta\lambda+4\sigma\beta_2\phi_d^2+\beta_1(-30\eta\lambda+4\beta_2\phi_d^4))))$$

$$\alpha_6 = -\frac{1}{2048\bar{\omega}^{12}(\bar{\omega}^2+\bar{\Omega}^2)^6\phi_d^6}243\varepsilon^2\eta\lambda\beta_2^3(30\eta\lambda\bar{\Omega}^2\beta_1^2-10\eta\lambda\beta_1^3+\bar{\Omega}^4(-30\eta\lambda\beta_1+\sigma\beta_2\phi_d^2)+\bar{\omega}^6(10\eta\lambda-\beta_2\phi_d^4)+\bar{\Omega}^6(10\eta\lambda-\beta_2\phi_d^4)+\bar{\omega}^4(6\alpha^2\eta\lambda-30\eta\lambda\beta_1+\sigma\beta_2\phi_d^2+\bar{\Omega}^2(30\eta\lambda-3\beta_2\phi_d^4))+\bar{\omega}^2(6\eta\lambda\beta_1(-\alpha^2+5\beta_1)+2\bar{\Omega}^2(3\alpha^2\eta\lambda-30\eta\lambda\beta_1+\sigma\beta_2\phi_d^2)+\bar{\Omega}^4(30\eta\lambda-3\beta_2\phi_d^4)))$$

$$\alpha_7 = \frac{2187\varepsilon^2\eta^2\lambda^2(5\bar{\omega}^4+\bar{\omega}^2(\alpha^2+10\bar{\Omega}^2-10\beta_1)+5(\bar{\Omega}^2-\beta_1)^2)\beta_2^4}{16384\bar{\omega}^{14}(\bar{\omega}^2+\bar{\Omega}^2)^6\phi_d^6}$$

$$\alpha_8 = -\frac{6561\varepsilon^2\eta^2\lambda^2(\bar{\omega}^2+\bar{\Omega}^2-\beta_1)\beta_2^5}{32768\bar{\omega}^{16}(\bar{\omega}^2+\bar{\Omega}^2)^6\phi_d^6}$$

$$\alpha_9 = \frac{6561\varepsilon^2\eta^2\lambda^2\beta_2^6}{262144\bar{\omega}^{18}(\bar{\omega}^2+\bar{\Omega}^2)^6\phi_d^6}$$

Appendix B

$$|\varphi_{10}| = N_{10}$$

$$|\varphi_{20}| = N_{20}$$

$$\nu_1 = \frac{27\varepsilon^4\eta^2\lambda^2N_{20}^4(\bar{\omega}^4+\bar{\omega}^2(\alpha^2+2\bar{\Omega}^2-2\beta_1)+(\bar{\Omega}^2-\beta_1)^2)}{256\bar{\omega}^8}+\frac{81\varepsilon^4\eta\lambda N_{10}^8\beta_2^3}{2048\bar{\omega}^{12}}-\frac{27\varepsilon^4\eta\lambda N_{10}^6(\bar{\omega}^2+\bar{\Omega}^2-\beta_1)\beta_2^2}{256\bar{\omega}^{10}}$$
$$-\frac{3\varepsilon^4\eta\lambda N_{20}^2(\bar{\omega}^4(\sigma+(-\alpha^2+\beta_1)\phi_d^2)+(\bar{\Omega}^2-\beta_1)(-\sigma\beta_1+\bar{\Omega}^2(\sigma+\beta_1\phi_d^2)))}{16\bar{\omega}^6}$$
$$-\frac{3\varepsilon^4\eta\lambda N_{20}^2(\bar{\omega}^2(\alpha^2\sigma-2\sigma\beta_1-\beta_1^2\phi_d^2+\bar{\Omega}^2(2\sigma-(\alpha^2-2\beta_1)\phi_d^2)))}{16\bar{\omega}^6}+\frac{1}{16\bar{\omega}^4}\varepsilon^2(\bar{\omega}^6(\gamma+\alpha\varepsilon\phi_d^2)^2$$
$$+\bar{\omega}^4(\alpha^2\gamma^2+\varepsilon^2\sigma^2-2\alpha^2\varepsilon^2\sigma\phi_d^2+\varepsilon^2\beta_1^2\phi_d^4+2\bar{\Omega}^2(\gamma+\alpha\varepsilon\phi_d^2)^2-2\beta_1(\gamma^2-\varepsilon^2\sigma\phi_d^2))$$
$$+\varepsilon^2(\sigma\beta_1-\bar{\Omega}^2(\sigma+\beta_1\phi_d^2))^2+\bar{\omega}^2(\alpha^2\varepsilon^2\sigma^2-2\varepsilon^2\sigma^2\beta_1+\bar{\Omega}^4(\gamma+\alpha\varepsilon\phi_d^2)^2+\beta_1^2(\gamma^2-2\varepsilon^2\sigma\phi_d^2)$$
$$+2\bar{\Omega}^2(\varepsilon^2\beta_1^2\phi_d^4+\varepsilon^2\sigma(\sigma-\alpha^2\phi_d^2)-\beta_1(\gamma^2-2\varepsilon^2\sigma\phi_d^2))))+N_{10}^2(-\frac{81\varepsilon^4\eta^2\lambda^2N_{20}^4(\bar{\omega}^2+\bar{\Omega}^2-\beta_1)\beta_2}{256\bar{\omega}^{10}}$$
$$-\frac{9\varepsilon^4\eta\lambda N_{20}^2\beta_2(2\sigma\beta_1+\bar{\omega}^4\phi_d^2+\bar{\Omega}^4\phi_d^2-2\bar{\Omega}^2(\sigma+\beta_1\phi_d^2)-2\bar{\omega}^2(\sigma-\bar{\Omega}^2\phi_d^2+\beta_1\phi_d^2))}{32\bar{\omega}^8}$$
$$+\frac{3\varepsilon^2\beta_2(\bar{\omega}^4(-\gamma^2+\varepsilon^2\sigma\phi_d^2+\varepsilon^2\beta_1\phi_d^4)-\varepsilon^2(\sigma-\bar{\Omega}^2\phi_d^2)(-\sigma\beta_1+\bar{\Omega}^2(\sigma+\beta_1\phi_d^2)))}{16\bar{\omega}^6}$$
$$+\frac{\bar{\omega}^23\varepsilon^2\beta_2(-\varepsilon^2\sigma^2+\beta_1(\gamma^2-2\varepsilon^2\sigma\phi_d^2)+\bar{\Omega}^2(-\gamma^2+2\varepsilon^2\sigma\phi_d^2+2\varepsilon^2\beta_1\phi_d^4))}{16\bar{\omega}^6})$$
$$+N_{10}^4(\frac{729\varepsilon^4\eta^2\lambda^2N_{20}^4\beta_2^2}{4096\bar{\omega}^{12}}+\frac{81\varepsilon^4\eta\lambda N_{20}^2\beta_2^2(-\sigma+\bar{\omega}^2\phi_d^2+\bar{\Omega}^2\phi_d^2)}{256\bar{\omega}^{10}}+\frac{1}{256\bar{\omega}^8}9\varepsilon^2\beta_2(\varepsilon^2\bar{\omega}^4(2\eta\lambda$$
$$+3\beta_2\phi_d^4)+\bar{\omega}^2(-2\alpha^2\varepsilon^2\eta\lambda-4\varepsilon^2\eta\lambda\beta_1+3\gamma^2\beta_2-6\varepsilon^2\sigma\beta_2\phi_d^2+2\varepsilon^2\bar{\Omega}^2(2\eta\lambda+3\beta_2\phi_d^4))$$
$$+\varepsilon^2(2\eta\lambda\beta_1^2+3\sigma^2\beta_2-2\bar{\Omega}^2(2\eta\lambda\beta_1+3\sigma\beta_2\phi_d^2)+\bar{\Omega}^4(2\eta\lambda+3\beta_2\phi_d^4))))$$

$$\nu_2$$
$$=-\frac{27\alpha\varepsilon^4\eta^2\lambda^2N_{20}^4\phi_d}{64\bar{\omega}^6}-\frac{27i\varepsilon^3\eta\lambda N_{10}^6(\bar{\omega}^2+\bar{\Omega}^2-\beta_1)\beta_2^2(1+\varepsilon\phi_d^2)}{128\bar{\omega}^9(\bar{\omega}^2+\bar{\Omega}^2)\phi_d}+\frac{81i\varepsilon^3\eta\lambda N_{10}^8\beta_2^3(1+\varepsilon\phi_d^2)}{1024\bar{\omega}^{11}(\bar{\omega}^2+\bar{\Omega}^2)\phi_d}$$
$$+\frac{9\varepsilon N_{10}^4\beta_2(i\varepsilon^2\eta\lambda\bar{\omega}^4+i\varepsilon^2\eta\lambda(\bar{\Omega}^2-\beta_1)^2-i\varepsilon^2\eta\lambda\bar{\omega}^2(\alpha^2-2\bar{\Omega}^2+2\beta_1)+3\gamma\bar{\omega}^3\beta_2+3\gamma\bar{\omega}\bar{\Omega}^2\beta_2)(1+\varepsilon\phi_d^2)}{64\bar{\omega}^7(\bar{\omega}^2+\bar{\Omega}^2)\phi_d}$$
$$-\frac{3\alpha\varepsilon^3\eta\lambda N_{20}^2\phi_d(-2\varepsilon\sigma+\bar{\omega}^2(1+\varepsilon\phi_d^2)+\bar{\Omega}^2(1+\varepsilon\phi_d^2))}{8\bar{\omega}^4}$$
$$-\frac{3\gamma\varepsilon N_{10}^2\beta_2(-2\beta_1(1+\varepsilon\phi_d^2)+\bar{\omega}^2(2+\varepsilon\phi_d^2+\varepsilon^2\phi_d^4)+\bar{\Omega}^2(2+\varepsilon\phi_d^2+\varepsilon^2\phi_d^4))}{8\bar{\omega}^4\phi_d}+\frac{1}{4\bar{\omega}^2\phi_d}\varepsilon(\gamma\beta_1^2-\alpha\varepsilon^3\sigma^2\phi_d^2+\gamma\varepsilon\beta_1^2\phi_d^2$$
$$+\bar{\omega}^4(\gamma+\alpha\varepsilon\phi_d^2)+\bar{\Omega}^4(\gamma+\alpha\varepsilon\phi_d^2)+\bar{\Omega}^2(\alpha\varepsilon^2\sigma\phi_d^2(1+\varepsilon\phi_d^2)-\gamma\beta_1(2+\varepsilon\phi_d^2+\varepsilon^2\phi_d^4))+\bar{\omega}^2(2\bar{\Omega}^2(\gamma+\alpha\varepsilon\phi_d^2)-\gamma\beta_1(2$$
$$+\varepsilon\phi_d^2+\varepsilon^2\phi_d^4)+\alpha(\alpha\gamma+\varepsilon(\alpha\gamma-\gamma^2+\varepsilon\sigma)\phi_d^2+\varepsilon^3\sigma\phi_d^4)))$$

$$\nu_3 = \frac{27\varepsilon^3\eta\lambda N_{10}^6(\bar{\omega}^2+\bar{\Omega}^2-\beta_1)\beta_2^2}{64\bar{\omega}^8(\bar{\omega}^2+\bar{\Omega}^2)^2} - \frac{81\varepsilon^3\eta\lambda N_{10}^8\beta_2^3}{512\bar{\omega}^{10}(\bar{\omega}^2+\bar{\Omega}^2)^2} + \frac{27\varepsilon^4\eta^2\lambda^2 N_{20}^4\phi_d^2}{64\bar{\omega}^6} + \frac{3\varepsilon^3\eta\lambda N_{20}^2(-\varepsilon\sigma+\beta_1)\phi_d^2}{4\bar{\omega}^4}$$
$$+ N_{10}^2\Big(\frac{9\varepsilon^3\eta\lambda N_{20}^2\beta_2\phi_d^2}{8\bar{\omega}^6}$$
$$- \frac{3\beta_2(-\beta_1 - 2\varepsilon\beta_1\phi_d^2 + \varepsilon^3\sigma\phi_d^4 - \varepsilon^2\beta_1\phi_d^4 + \bar{\omega}^2(1+\varepsilon\phi_d^2+\varepsilon^2\phi_d^4) + \bar{\Omega}^2(1+\varepsilon\phi_d^2+\varepsilon^2\phi_d^4))}{4\bar{\omega}^4\phi_d^2}\Big)$$
$$+ \frac{1}{4\bar{\omega}^2\phi_d^2}(\bar{\omega}^4+\bar{\Omega}^4+\beta_1^2+2\varepsilon\beta_1^2\phi_d^2+\varepsilon^4\sigma^2\phi_d^4-2\varepsilon^3\sigma\beta_1\phi_d^4+\varepsilon^2\beta_1^2\phi_d^4-2\bar{\Omega}^2\beta_1(1+\varepsilon\phi_d^2+\varepsilon^2\phi_d^4)$$
$$+ \bar{\omega}^2(\alpha^2+2\bar{\Omega}^2+2\alpha^2\varepsilon\phi_d^2-4\alpha\gamma\varepsilon\phi_d^2+\alpha^2\varepsilon^2\phi_d^4-2\alpha\gamma\varepsilon^2\phi_d^4+\gamma^2\varepsilon^2\phi_d^4-2\beta_1(1+\varepsilon\phi_d^2+\varepsilon^2\phi_d^4)))$$
$$+ \frac{1}{64\bar{\omega}^6(\bar{\omega}^2+\bar{\Omega}^2)^2\phi_d^2}9N_{10}^4\beta_2(4\varepsilon^3\eta\lambda\bar{\Omega}^2\beta_1\phi_d^2-2\varepsilon^3\eta\lambda\beta_1^2\phi_d^2+\bar{\omega}^4(-2\varepsilon^3\eta\lambda\phi_d^2+3\beta_2(1+\varepsilon\phi_d^2)^2)$$
$$+ \bar{\Omega}^4(-2\varepsilon^3\eta\lambda\phi_d^2+3\beta_2(1+\varepsilon\phi_d^2)^2)+2\bar{\omega}^2(\varepsilon^3\eta\lambda(\alpha^2+2\beta_1)\phi_d^2+\bar{\Omega}^2(-2\varepsilon^3\eta\lambda\phi_d^2$$
$$+ 3\beta_2(1+\varepsilon\phi_d^2)^2)))$$

$$\nu_4 = -\frac{\alpha}{\phi_d} + (-\alpha+\gamma)\varepsilon\phi_d$$